PFC/JA-87-32

Stabilization of Sawteeth By Lower Hybrid Waves in the Alcator C. Tokamak

S. Knowlton, M. Porkolab, Y. Takase

Plasma Fusion Center
Massachusetts Institute of Technology
Cambridge, MA 02139

September 1987

Submitted to: Nuclear Fusion

This work was supported by the U. S. Department of Energy Contract No. DE-AC02-78ET51013. Reproduction, translation, publication, use and disposal, in whole or in part by or for the United States government is permitted.

Stabilization of Sawteeth by Lower Hybrid Waves in the Alcator C Tokamak

S. Knowlton[†], M. Porkolab, and Y. Takase

Plasma Fusion Center
Massachusetts Institute of Technology
Cambridge, MA 02139

ABSTRACT

Sawteeth have been suppressed by lower hybrid current drive in high density Alcator C plasmas. At a density of $1.1 \times 10^{14}\text{cm}^{-3}$ and $q(a) = 4.7$ the sawteeth were eliminated by application of $P_{rf} = 600$ kW at 4.6 GHz, which represents an estimated 30% of the rf power required to fully sustain the discharge in the absence of ohmic power. Strong electron heating is observed with both current drive and anti-current drive phasings of the waveguide arrays but sawtooth stabilization occurs only in the former case. For the current drive phasing, the sawtooth period increases with rf power until the sawteeth are stabilized, while the period remains unchanged for rf injection with anti-current drive phasing. The internal inductance of the plasma increases during current drive relative to the anti-current drive case. The disappearance of sawteeth and the increase in internal inductance suggests that the rf current is driven near the q = 1 surface. At high power ($P_{rf} > 850$ kW), the sawteeth return $40 - 60$ ms into the rf pulse, indicating that an optimal power range, or rf deposition profile, exists for successful sawtooth suppression.

I. Introduction

The possibility of suppressing the sawtooth instability, particularly in high density, reactor-grade plasmas has recently attracted interest because of substantial electron energy losses associated with giant sawteeth in ICRF-heated plasmas [1]. It is expected that by eliminating large sawteeth, the average critical electron temperature will increase and concurrently the central electron energy confinement will be significantly improved. Furthermore, the theoretical understanding of sawtooth behavior is presently being re-evaluated [2,3] as a result of recent experimental studies of sawteeth on large tokamaks [4]. The ability to modify and suppress sawteeth by lower hybrid current drive (LHCD) may shed light on details of the sawtooth generation mechanism in conventional ohmic or auxiliary-heated plasmas. In addition, our understanding of MHD stability in toroidal geometry may be aided by these experiments.

Suppression of sawteeth by lower hybrid waves has been reported in current-driven plasmas in which all or part of the current is driven by lower hybrid waves [5-9]. In all cases, the sawteeth are suppressed when sufficient rf power is launched in the current drive mode, namely with the waveguide grill phased to launch a traveling wave spectrum predominantly in the direction of the electron drift. In low density Petula and Asdex experiments [6,8], the internal inductance is observed to decrease during rf current drive experiments. This suggests that the radial current profile has flattened and sawtooth stabilization is achieved when the safety factor $q(r)$ rises above unity everywhere in the plasma. In the Asdex experiments, the current density profile was measured directly, and the results corroborated the magnetic measurements. In these cases, sawtooth suppression was explained by the elimination of the q = 1 surface everywhere in the plasma. However, in the PLT low density experiments when sawteeth were suppressed, a residual $m = 1$ oscillation was often observed, suggesting that the q = 1 surface may still have been present at rf powers sufficient to stabilize the sawteeth. However, at higher rf powers the $m = 1$ oscillation was also eliminated [7]. Sawteeth have also been suppressed by lower hybrid current drive in considerably higher density plasmas [6,9]. The Petula experiments

are noteworthy because of the wide density range ($\bar{n}_e = 1 - 8 \times 10^{13}$ cm^{-3}) over which stabilization could be achieved, and the Alcator C experiments are of interest because of the reactor relevant conditions during stabilization ($\bar{n}_e \simeq 1 \times 10^{14}$cm^{-3}, B $\sim$ 6 T). Of particular interest are differences in the sawtooth behavior and the evolution of $\beta_p + \ell_i/2$ between low and high density plasmas. In this paper, we report results of stabilization experiments in the Alcator C tokamak by lower hybrid current drive at high densities.

II. Experimental Results on Sawtooth Stabilization

The stabilization studies on Alcator C ($R_0 = 64$cm, a = 16.5 cm, molybdenum limiter) were performed at $B_\phi = 6$ T, $q(a) = 4-6$, $\bar{n}_e = 0.6-1.2\times10^{14}$cm^{-3} in both hydrogen and deuterium discharges. Microwave power at 4.6 GHz was coupled to the plasma through either two or three 16-waveguide arrays, with a total net power up to $P_{rf} = 1.4$ MW at $I_p = 260$ kA, $q(a) = 4.7$, $\bar{n}_e = 1.1 \times 10^{14}$ cm^{-3} for current drive phasing (relative phase between adjacent waveguides $\Delta\phi = +90°$). Substantial electron and ion heating is observed during rf injection in Alcator C for most waveguide phasings [9]. In order to distinguish between the effects of bulk heating and current drive, we compare the sawtooth behaviour during rf injection for both $\Delta\phi = +90°$ (current drive) and $-90°$ (anti-current drive phasing) with the same spectrum. The electron temperature was obtained with either a 5-channel ruby Thomson scattering system or, in later experiments, with a single-channel multi-shot Nd-Yag system. Ion temperatures were measured by analysis of charge-exchange neutrals emitted by the plasma.

In Fig. 1 the increase in central electron and ion temperatures vs rf power are shown for $I_p = 270$ kA, $\bar{n}_e = 0.7 - 0.8 \times 10^{14}$ cm^{-3}, $T_{eo}^{ohmic} = 1.3$ keV, $T_{io}^{ohmic} = 0.75$ keV. The solid symbols represent discharges in which the sawteeth are stabilized. While the temperature increases are comparable in both cases, the electron temperature is somewhat lower and the ion temperature higher for the current drive ($\Delta\phi = 90°$) phasing.

The major diagnostic of sawtooth behavior is a 16-channel soft x-ray diode array which is sensitive in the range $1.5 - 15$ keV. The central chord soft x-ray emission is shown

in Fig. 2 for two shots for nearly equal rf powers, one at $\Delta\phi = +90°$ and the other at $\Delta\phi = -90°$. While the sawteeth are still present in the anti-current drive case, they are entirely suppressed for the LHCD phasing. The apparent residual oscillations at a frequency of 360 Hz result from plasma horizontal motion due to equilibrium field power supply ripple. The large increase in the soft x-ray signal during rf injection is caused largely by an influx of molybdenum ions from the limiters and by formation of the high energy electron tail. Based on spectroscopic measurements of the edge state molybdenum line emission, the molybdenum impurity source rate doubles during rf injection with current drive phasing ($\Delta\phi = 90°$) at a power sufficient to stabilize the sawteeth, and increases by a factor of $3-4$ for anti-current drive phasing ($\Delta\phi = -90°$) at the same rf power. While the central molybdenum densities inferred from spectroscopy are less certain, the central state emission is nonetheless higher in the anti-current drive case than for current drive phasing. The increase in Z_{eff}, measured by visible Bremsstrahlung, is approximately 0.3 in both cases.

The period between sawteeth generally increases during rf injection. The sawtooth period vs rf power is plotted in Fig. 3 for $\Delta\phi = +90°, -90°$ and $180°$. For these plasma conditions, the sawteeth are usually stabilized for $\Delta\phi = +90°$ and $P_{rf} \gtrsim 550$ kW; however, some shots above this threshold power did not fully stabilize and their sawtooth periods are also plotted. The sawtooth period increases to at most twice its initial value for $\Delta\phi = +90°$ phasing, while for $-90°$ phasing the sawtooth repetition time rises only by a modest amount. In contrast to low density stabilization experiments on PLT and Asdex [7,8], the sawtooth period increases monotonically with rf power, and does not decrease for rf powers just below the stabilization threshold. The sawtooth inversion radius inferred from the soft x-ray profile data does not differ substantially from the inversion radius in ohmic plasma for any phasing or rf power level at which sawteeth are still observed. The loop voltage is observed to drop during rf injection from its initial value of $V_\ell = 1.5$ V to values as low as $V_\ell \simeq 0.5$ V. As shown in Fig. 4, the loop voltage drop is larger for the case of $\Delta\phi = +90°$ than for other phasings; moreover, the decrease in loop voltage for sawtooth-stabilized shots is somewhat greater than for those at similar rf power which did not stabilize. Again, while a fraction of the loop voltage drop can be explained by

bulk plasma heating, the difference between $\Delta\phi = +90°$ and $-90°$ cases indicates that a significant fraction of the total plasma current for $\Delta\phi = +90°$ is carried by suprathermal electrons. The correlation of the magnitude of the loop voltage drop with the suppression of sawteeth also suggests that the operative condition for sawtooth stabilization is, for given plasma conditions, the appropriate fraction of rf driven current.

Because of the large change in the overall level of the soft x-ray emission during rf injection, the amplitude of the sawteeth on the soft x-ray signal in itself is not an accurate indicator of the intensity of the sawtooth activity in the plasma. Instead, we find the width of the soft x-ray profile, particularly the change in profile width during a sawtooth, to be a sensitive measure of the strength of the sawtooth behavior. Prior to rf injection, the soft x-ray profile half-width (based on a nearly gaussian fit to the soft x-ray data) typically increases from 3 cm to a value of 5 cm during the sawtooth crash. When the sawteeth are entirely suppressed, the x-ray width remains constant at a value comparable to or somewhat narrower than the width in the ohmic plasma just prior to the sawtooth crash, as shown in Fig. 5. At power levels just below the stabilization threshold, the sawtooth activity is still present, although the amplitude is reduced from the ohmic level. For $\Delta\phi = -90°$, the sawtooth intensity is unchanged during rf injection.

III. Magnetic Measurements

While the current density profile has not been measured directly in these experiments, qualitative information can be obtained from measurements of the equilibrium quantity $\beta_p + \ell_i/2$, where β_p is the poloidal beta and ℓ_i is the internal inductance parameter. During rf injection, $\beta_p + \ell_i/2$ increases for both $\Delta\phi = +90°$ and $-90°$. Typical traces for both phasings at similar rf power levels are shown in Fig. 6. Due to offset errors in the measurement, the absolute value in $\beta_p + \ell_i/2$ is not reliable, but relative measurements remain valid. In direct contrast to the low density Asdex results [8], the increase in the quantity $\beta_p + \ell_i/2$ is approximately a factor of 3 higher for the LHCD case than that of anti-current drive. The increase in $\beta_p + \ell_i/2$ vs rf power is plotted in Fig. 7. While $\beta_p + \ell_i/2$ rises monotonically with rf power, it appears that there is a large change in $\beta_p + \ell_i/2$ at

relatively low rf power levels, at least for the case of $\Delta\phi = +90°$. The increase in $\beta_p + \ell_i/2$ in the $\Delta\phi = 90°$ shots is not coincident with sawtooth stabilization but increases smoothly with rf power for $P_{rf} \geq 175$ kW. The increase in $\beta_p + \ell_i/2$ is larger for $\Delta\phi = +90°$ than for $\Delta\phi = -90°$ at all power levels. We have estimated the contribution of the observed bulk heating to β_p and concluded that for $P_{rf} \simeq 500 - 600$ kW, $\Delta\beta_p^{th} \simeq 0.04 - 0.05$ above the initial ohmic value of 0.18-0.20. The remainder of the increase must result from a change in internal inductance and/or an additional increase in β_p resulting from the energy stored in the suprathermal electron tail.

While the stored energy in the tail has not been measured directly in these experiments, as was done in pure LHCD plasmas in Alcator [10], we have compared the hard x-ray Bremmstrahlung emission profiles from the suprathermal tail for both phasings to obtain a relative indication of the energy stored in the tail [11]. The x-ray emission in the range $E_\gamma = 30$-500 keV is measured with an 8-channel array viewing the plasma perpendicularly. For photons of energy $E_\gamma = 40 - 160$ keV, both the intensity and the radial profiles of the emission are similar for $\Delta\phi = +90°$ and $-90°$. Similar to observations in pure LHCD experiments [10], the emission profile is more peaked for low energy x-ray photons than for high energy ones. Because of the reduced accessibility in the present experiments (lower magnetic fields and higher densities than in Ref. [10]) the emission profiles are typically broader than for pure LHCD plasmas, particularly for the high energy photons. The mean energy of the x-ray distribution increases with radius, indicating that the fastest electrons are located off-axis. Based on our measurements, we conclude that the energy stored in the electron tail is comparable for both phasings. Thus, the difference in the measurements of $\beta_p + \ell_i/2$ may be explained by an increase in internal inductance for $\Delta\phi = +90°$ relative to the case of $\Delta\phi = -90°$.

The conclusion that the internal inductance increases for $\Delta\phi = +90°$ (current drive) is further supported by a comparison of the time evolution of the $\beta_p + \ell_i/2$ signals in Fig. 6. The trace for the LHCD phasing ($\Delta\phi = +90°$) rises over a 20-30 msec period and increases slowly over the remainder of the rf pulse. Following rf shut-off, it decays rapidly at first, and then more slowly for the remaining 50 msec of the discharge. In contrast,

the trace for $\Delta\phi = -90°$ rises to its peak value in approximately 10 msec, decreases very slowly during the rf pulse, and drops rapidly at rf shut-off. The expected time interval for the evolution of the tail due to rf-generated diffusion is on the order of 1 msec, while that for the bulk thermal energy is about 8 msec. These characteristic times are similar to the fast evolution of the $\beta_p + \ell_i/2$ signal, while the slower evolution may represent the resistive diffusion time, calculated to be typically 50 msec for the inner half of the plasma. Based on these comparisons of the time evolution and on our estimates of thermal and tail β_p for the two phasings, we conclude that the inductance is higher in the $\Delta\phi = +90°$ case than for the opposite phasing by approximately 0.05. We also conclude that for the LHCD phasings, the internal inductance increases above the value in the ohmic plasma.

IV. Suppression of Sawteeth at High Powers

Regarding the timing of the suppression of sawteeth in relation to the rf pulse, we often observe an interesting evolution of the sawtooth behavior during the rf pulse. At rf power levels below which stabilization is achieved, e.g. $P_{rf} < 400$ kW, the sawtooth activity is nearly suppressed early in the pulse, (judging from the reduction of the amplitude of the x-ray profile width), but increases during the rf pulse to become comparable to the amplitude of the ohmic sawteeth. Furthermore, we have found in earlier experiments [9] that at rf power levels significantly higher than that required to stabilize the sawteeth for the entire pulse, the sawteeth can recur during the rf pulse after a stable period of 40-70 msec into the pulse. For plasma parameters $I_p = 265$ kA, $B_T = 6.2$ T, $\bar{n}_e = 1.1 - 1.2 \times 10^{14}$ cm^{-3}, the sawteeth are stabilized at an input rf power of $P_{rf} \gtrsim 600$kW. Based on an extrapolation from pure LHCD experiments on Alcator C [12], this power threshold represents approximately $20 - 30\%$ of the estimated rf power required to fully drive these discharges with rf current alone. In this case, the loop voltage drops by 0.55 V, or approximately 30% of the ohmic value. Above this lower rf power threshold value, the sawteeth are stabilized for the entire 100 msec duration of the pulse at rf power levels $P_{rf} \lesssim 850$ kW. Above this second power level up to the maximum power of $P_{rf} = 1.3$ MW, the sawteeth are initially stabilized; however after a typical interval of 20-30 msec, a high

frequency, odd harmonic (presumably m = 1) oscillation is observed on the central soft x-ray channels. Simultaneously, the soft x-ray profile broadens as shown in Fig. 8. The oscillations last for an additional 20-30 msec after which the sawtooth oscillations return.

The amplitude of the sawteeth oscillations, as measured by the average change in the soft x-ray profile width during the sawtooth is plotted as a function of rf power in Fig. 9. (Here, a different method was used to quantify the x-ray profile width resulting in somewhat different numerical values). At rf power levels below $P_{rf} = 600$ kW, the sawtooth intensity is reduced by LHCD. For $P_{rf} \geq 850$ kW, the sawtooth intensity increases with rf power and at $P_{rf} \sim 1.3$ MW the sawtooth activity after the initial stabilization is comparable to the pre-injection level.

The loop voltage drop for this rf power scan is plotted in Fig. 10. Although the value of the loop voltage drop appears to saturate at high rf powers, the reduction of loop voltage for the shots in which the sawteeth are initially stabilized but later recur is comparable with, or even larger than that for lower power shots in which the sawteeth are stabilized for the entire rf pulse. Thus the fraction of rf driven current is larger for the high power shots than for the low power ones.

In general, the onset of the $m = 1$ oscillation is not always followed by the recurrence of the sawteeth: at lower rf powers a saturated mode is often found to persist for the entire duration of an rf pulse in which the sawteeth are suppressed. The radial location of the oscillation extends across the inversion radius of the pre-injection plasma. Similar oscillations are sometimes observed superimposed on sawteeth at power levels below the stabilization threshold. In short, we have observed under certain conditions that there is an optimal rf power level for the stabilization of sawteeth. Although the cause of this phenomenon is not fully understood, it is plausible that the rf deposition profile, and hence the fast electron current profile and rf heating profile may vary with rf power as the plasma parameters evolve during the rf pulse. The frequent observations of $m = 1$ oscillations in our experiments suggests that the LHCD current profile may be "barely" stable, and that a slight change in the imposed rf current profile may be sufficient to cause

instability. We remark that in cases in which the sawteeth return during the pulse, the measured value of $\beta_p + \ell_i/2$ is nearly the same in the stabilized and unstabilized portion of the rf pulse; therefore we cannot invoke a significant change in the current profile to explain the recurrence of the sawteeth. These results suggest that not only is the fraction of the total current carried by the rf-driven suprathermal electrons important to achieve sawtooth stabilization but the deposition profile also influences the ability to suppress the sawteeth.

V. Discussion and Summary

According to conventional MHD theory, sawtooth stabilization can be achieved by a careful tailoring of the toroidal current profile so that $q(r) > 1$ everywhere in the plasma. This usually requires a decoupling of the electron temperature and the toroidal current profiles in a initially unstable ($q(0) < 1$) plasma. In the usual case such a situation is achievable by driving additional currents by lower hybrid waves in the outer plasma layers so that the central current density is reduced (since the total current is conserved) [8]. By driving sufficiently large amounts of surface current, the total current profile broadens by diffusion and stability is achieved when $q(r) \gtrsim q(0) > 1$. The broadening of the current profile usually manifests itself by a decreasing internal inductance [8]. In principle, higher rf powers and larger edge currents result in higher values of $q(0)$ and therefore greater stability. One potential problem with driving edge currents indiscriminantly is the excitation of $m = 2$ modes which may lead to disruptions [6].

The present experimental results differ from this conventional picture in at least two regards: (a) As the power is raised the self inductance increases, yet the sawteeth are stabilized; (b) sawteeth are stabilized only for a certain range of injected powers and rf driven currents. In particular, at very high powers, the sawteeth recur after a few tens of milliseconds. It is further noted from Fig. 2 that the time delay between the start of the rf pulse and the suppression of the sawteeth is only a few milliseconds, as is the time interval for the return of the sawteeth following the shut-off of the rf power. It is apparent from these experimental results that stabilization is achieved by subtle changes

in the radial current density profile which results from a balance between rf driven and inductively driven currents, in which the diffusion of rf driven current or minor changes in rf deposition profile may play a role. We find that it is possible to construct model current profiles which are in agreement with the measured inductances and inversion radius, and also exhibit a rise in the central value of q above unity. In particular, the present results can be modelled by assuming that the rf driven current is generated in the plasma interior, specifically near the $q(r) = 1$ radial position, rather than in the plasma periphery. In such a case, the current in the plasma periphery ($r > a/2$) is reduced, and a current pedestal around the $q(r) = 1$ layer may be formed. It is easy to show that in such a case the internal inductance is increased, in agreement with experimental observations. The behavior near the plasma axis is difficult to predict. In particular, $q(0) < 1$ may be the appropriate condition at low to intermediate rf powers. The competition between diffusion of the rf currents and the slowing down of fast electrons, as well as plasma heating must be included in a realistic modeling of these results.

A detailed study of these phenomena have been undertaken using the Bonoli lower hybrid ray tracing code which includes a Fokker-Planck calculation for the fast electron tail and plasma transport modelling [13-15]. The appropriate parallel wave number power spectrum corresponding to our launcher geometry was used; current drive ($\Delta\phi = 90°$), anti-current drive ($\Delta\phi = -90°$) and heating spectra (180°) were studied. In general, reasonable agreement with the experiments was obtained for all phasings. In particular, it was found that for the current drive phasing the rf current was generated near the $q(r) = 1$ surface, roughly in agreement with the model discussed above. Thus, the total current was reduced at large radii ($r > 0.6a$) and the internal inductance increased. However, as the rf power was raised above $\sim$ 500 kW, a flat plateau developed in the total current, with $q(r) \simeq 1.0$ for radii in the range $0.2a \lesssim r \lesssim 0.3$ a. The central $q(0)$ values were close to unity, but usually $q(0) < 1.00$ at low to intermediate powers ($P < 1$ MW). In this case, the stability may have been achieved by mechanisms suggested by recent predictions of fully toroidal MHD codes, such as that that by Hender et al [16]. The stability of the generated current profiles are being studied presently with MHD codes. As the rf power was increased to high powers ($P_{RF} > 1$ MW), in our ray tracing and transport

simulations, $q(0)$ rose above unity initially, but off-axis, the value of q was lowered below unity because of strong localized current drive. Thus, the $q(r) = 1.0$ boundary was crossed at two locations r_1 and r_2, and instability would be once again expected. Therefore it appears that the key element in the present stabilization experiments is a flattening of the current profiles near the $q = 1$ surface at medium power levels, and initially at high powers. Ultimate stability, and whether $q(0)$ is greater or less then unity depends on the exact balance between diffusion of rf currents and inductive fields, as well as the evolution of other plasma parameters, including collisional slowing down of fast electrons. It is hoped that by combining the rf current drive modelling with a fully toroidal MHD code some of these issues can be resolved. Finally, it should be noted that similar current profiles have been invoked in ohmic plasmas in the Textor tokamak [16,17] to explain the relatively stable operating parameter space.

In summary, the present experiments demonstrate the possibility of decoupling temperature and partially rf driven current profiles in subtle ways. Further studies along these lines may help us to find new, and perhaps more efficient ways to stabilize MHD modes in a toroidal plasma (it is estimated that in the present experiments $I_{RF}/I_{Total} \sim 0.2$ when stabilization is achieved). Furthermore, these studies should help to improve our understanding of the MHD stability of toroidal plasma systems, as well as elucidate the limitations of partially toroidal MHD models versus fully toroidal MHD codes that have gained favor in recent studies.

Acknowledgements

We are grateful for the rf engineering support of D. Griffin and the support and assistance of the Alcator C operating staff. Thanks also go to S. McCool and R. Watterson for Thomson scattering measurements, J. Squire and S. Texter for hard x-ray measurements, J. Terry for spectroscopic impurity studies, R. Granetz for providing the soft x-ray array, M. Greenwald for help in the soft x-ray analysis, C. Fiore for charge exchange measurements, and F.S. McDermott for machine operations. We finally acknowledge a great deal of work by P. Bonoli on the modelling of the experimental results.

Work supported by U.S. Department of Energy Contract No. DE-AC02-78ET51013.

† Present address: JET Joint Undertaking, Abingdon, Oxon, England.

REFERENCES

[1] Jacquinot, J., Anderson, R.J., Arbez, J., Bartlett, D., Beaumont, B., et al., Plasma Phys. and Cont. Fusion 28 (1986) 1; Lallia, P.P., Ainsworth, A., Altmaim, H., Anderson, R.J., Arbez, J., et al., Plasma Phys. Control. Fusion 28 (1986) 1211.

[2] Wesson, J. A., Plasma Phys. and Cont. Fusion 28 (1986) 243.

[3] Denton, R. E., Drake, J. F., Kleva, R. G., and Boyd, D. A., Phys. Rev. Lett. 56 (1986) 2477.

[4] Edwards, A.W., Campbell, D.J., Engelhardt, W.W., Fahrback, H.U., Gill, R.D., et al., Phys. Rev. Lett. 57 (1986) 210; Campbell, D.J., Gill, R.D., Gowers, C.W., Wesson, J., Bartlett, D.V., et al., Nucl. Fusion 26 (1986) 1085.

[5] van Houtte, D., Briffod, G., Chabert, P., Gormezano, C., How, J., et al., Nucl. Fusion 24 (1984) 1485.

[6] van Houtte, D., Agarici, C., Bottolier-Curtit, H., Briand, P., et al., in Controlled Fusion and Plasma Physics, (Proc. 13th Eur. Conf., Schliersee, 1986) Vol. II (1986) 331.

[7] Chu, T-K., Bell, R., Bermabei, S., Cavallo, A., Guharay, S., et al., Nucl. Fusion 26 (1986) 666.

[8] Söldner, F., McCormick, K., Eckhartt, D., Kornher, M., Leuterer, F., et al., Phys. Rev. Lett. 57 (1986) 1137. Also, McCormick, K., Söldner, F.X., Eckhardt, D., Leuterer, F., Murmann, H., et al., Phys. Rev. Lett. 58 (1987) 491.

[9] Porkolab, M., Knowlton, S., Takase, Y., Texter, S., Bonoli, P., et al., in Controlled Fusion and Plasma Physics, (Proc. 13th Eur. Conf., Schliersee, 1986) Vol. II (1986) 445.

[10] Texter, S., Knowlton, S., Porkolab, M., and Takase, Y., Nucl. Fusion 26 (1986) 1279.

[11] Stevens, J., von Goeler, S., Bernabei, S., Bitter, M., Chu, T.K., et al., Nucl. Fusion 25 (1985) 1529.

[12] Porkolab, M., Schuss, J.J., Lloyd, B., Takase, Y., Texter, S., et al., Phys. Rev. Lett. 53 (1984) 450.

[13] Bonoli, P.T., and Englade, R.C., Phys. Fluids, 29 (1986) 2937.

[14] Bonoli, P.T., and Porkolab, M., Sherwood Theory Meeting, 1987, San Diego, CA.

[15] Bonoli, P.T., 7th APS topical conference on Applications of RF Power to Plasmas, Paper A-1, Kissimmee, Fl, 1987 [to be published].

[16] Hender, T.C., Robinson, D.C., and Snipes, J.A., 11-th Int. Conf. on Plasma Physics and Contr. Nucl. Fusion Res., Kyoto, Japan, 1986, paper IAEA-CN-47/A-V-3.

[17] Hender, T., (1987) private communication; also to be published in Controlled Fusion and Plasma Physics (Proc. 14th Eur. Conf., Madrid, 1987).

Figure Captions

1. Increase in the central electron and ion temperatures for current drive ($\Delta\phi = +90°$) and anti-current drive ($\Delta\phi = -90°$) plasmas vs. P_{rf} for $\bar{n}_e = 0.7 - 0.9 \times 10^{14}$ cm^{-3} and $q(a) = 4.7$. The solid symbols represent shots in which stabilization of sawteeth is observed.

2. Central chord measurement of the soft x-ray emission for $B_T = 6.0$ T, $I_p = 270$ kA, $\bar{n}_e = 0.8 \times 10^{14}$ cm^{-3}. (a) $\Delta\phi = +90°$, $P_{rf} = 590$ kW; (b) $\Delta\phi = -90°$, $P_{rf} = 600$ kW.

3. Average sawtooth period vs. net rf power for the current drive and anti current drive phasing, as well as for several shots at symmetric phasing ($\Delta\phi = 180°$). The plasma conditions are the same as in Fig. 1.

4. The loop voltage drop during the rf pulse vs. P_{rf} for $\Delta\phi = +90°, -90°$, and 180°; same conditions as in Fig. 1. The solid symbols indicate the sawtooth - stabilized shots. The loop voltage prior to the rf is 1.5 V.

5. The half-width of the soft x-ray radial profile vs. time for the current drive phasing, $\bar{n}_e = 0.7 \times 10^{14}$ cm^{-3}, $q(a) = 4.7$, $P_{rf} = 620$ kW.

6. The value of $\beta_p + \ell_i/2$ deduced from magnetic equilibrium measurements for the current drive phasing (solid line) and anti-current drive (dashed line) for the same conditions as in Fig. 2.

7. The increase in Λ ($\Lambda \equiv \beta_p + \ell_i/2 - 1$) vs. P_{rf} for the same conditions as in Fig. 1.

8. (a) Central chord measurement of the soft x-ray emission for current drive phasing at $P_{rf} = 1.05$ MW, $B_T = 6.3$ T, $I_p = 265$ kA, and $\bar{n}_e = 1.1 \times 10^{14}$ cm^{-3}. The thick line following the peak emission represents $m = 1$ oscillations. (b) Soft x-ray profile half width.

9. Intensity of the sawtooth oscillation, as indicated by the variation in the soft x-ray profile width during the sawtooth vs. rf power for the current drive phasing; B_T = 6.2 T, I_p = 265 kA, and $\bar{n}_e = 1.1 - 1.2 \times 10^{14}$ cm^{-3}. The arrow labelled P_{OH} indicates the ohmic power prior to injection.

10. The drop in loop voltage vs. P_{rf} for the same conditions as in Fig. 10. The initial loop voltage is 1.5 V.

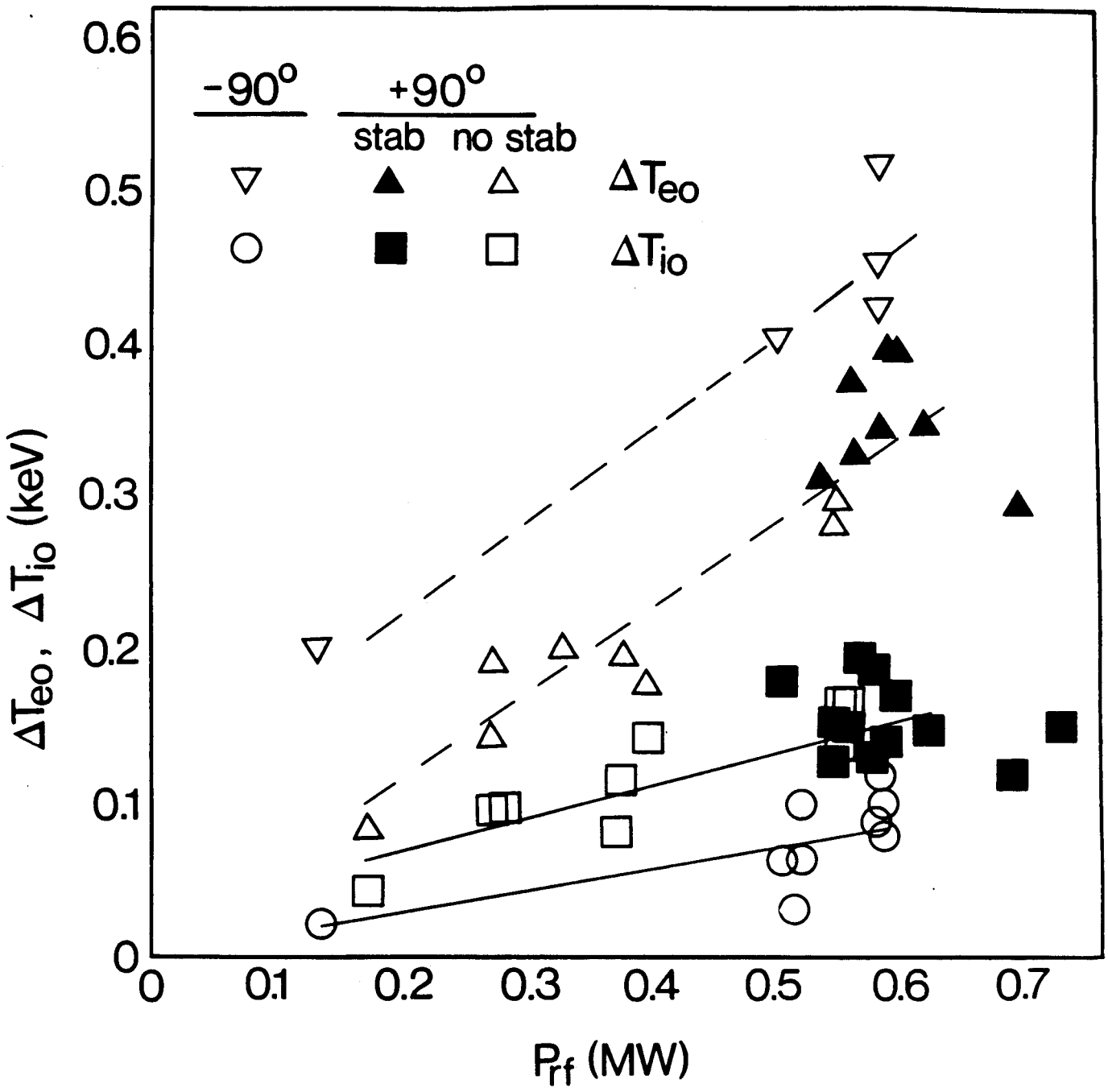
-90°
+90°
stab
no stab
ΔTeo
ΔTio
0.6
0.5
0.4
0.3
0.2
0.1
0
0
0.1
0.2
0.3
0.4
0.5
0.6
0.7
ΔTeo, ΔTio (keV)
Prf (MW)

Figure 1

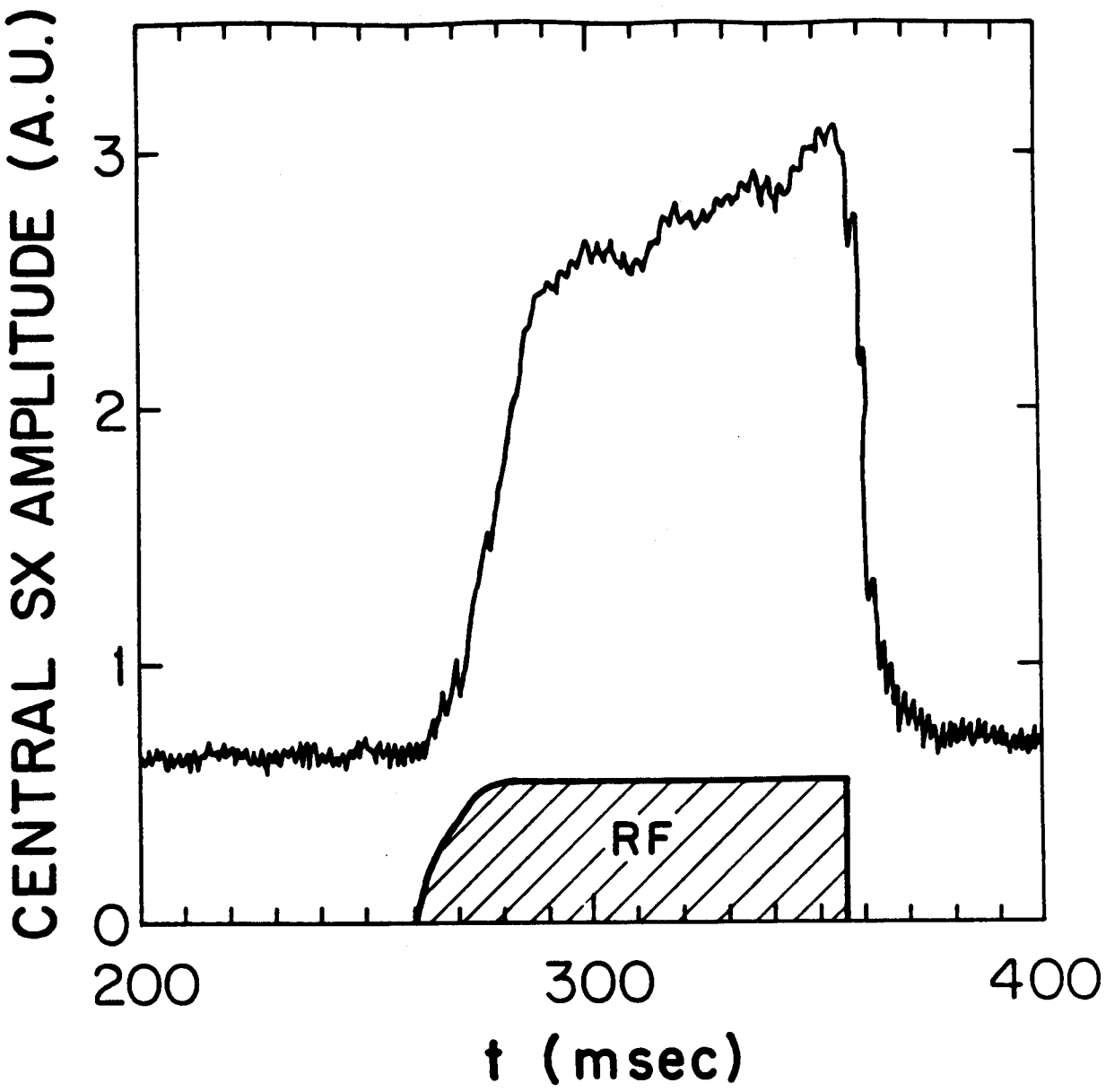

Figure 2a

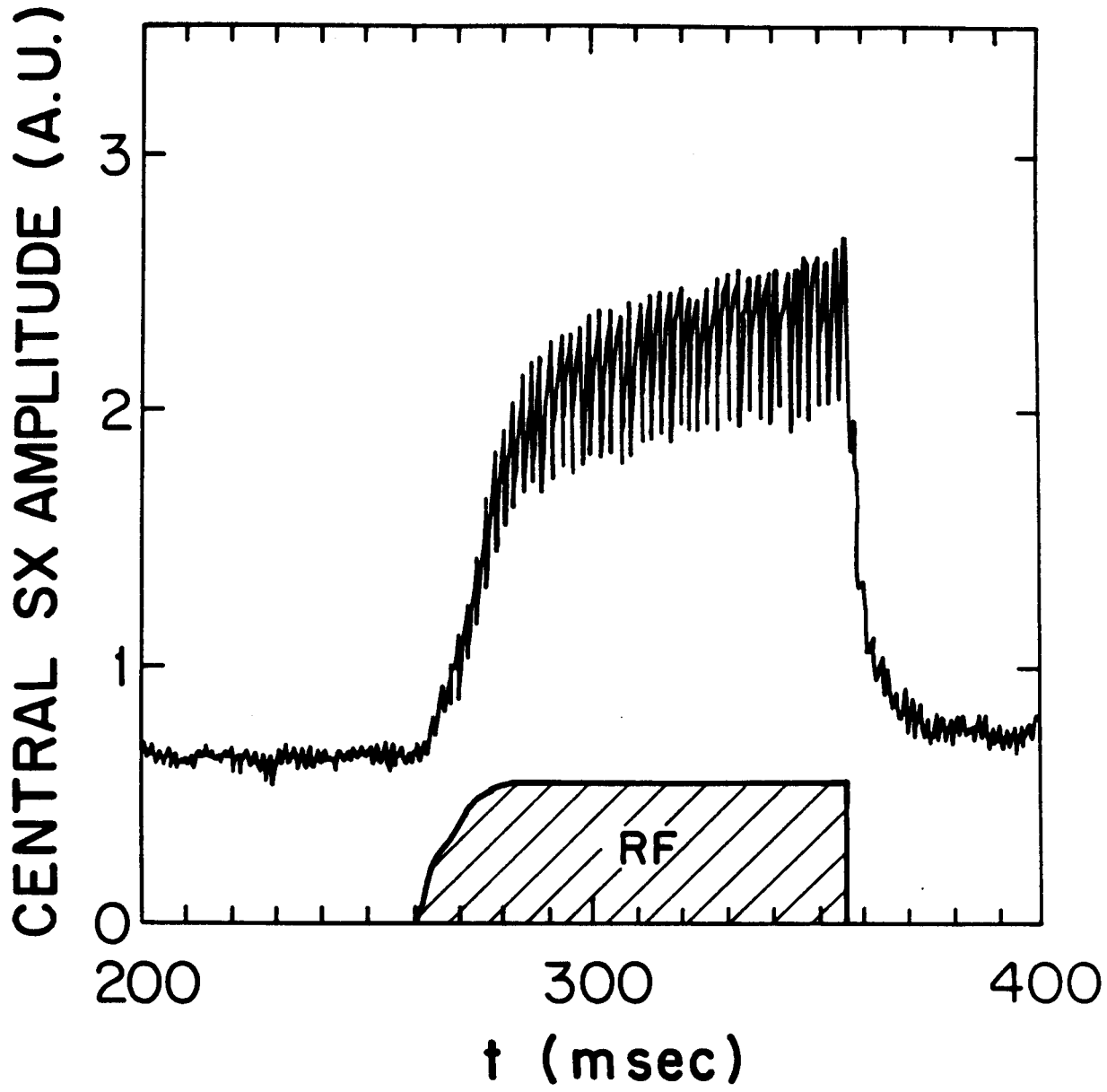

Figure 2b

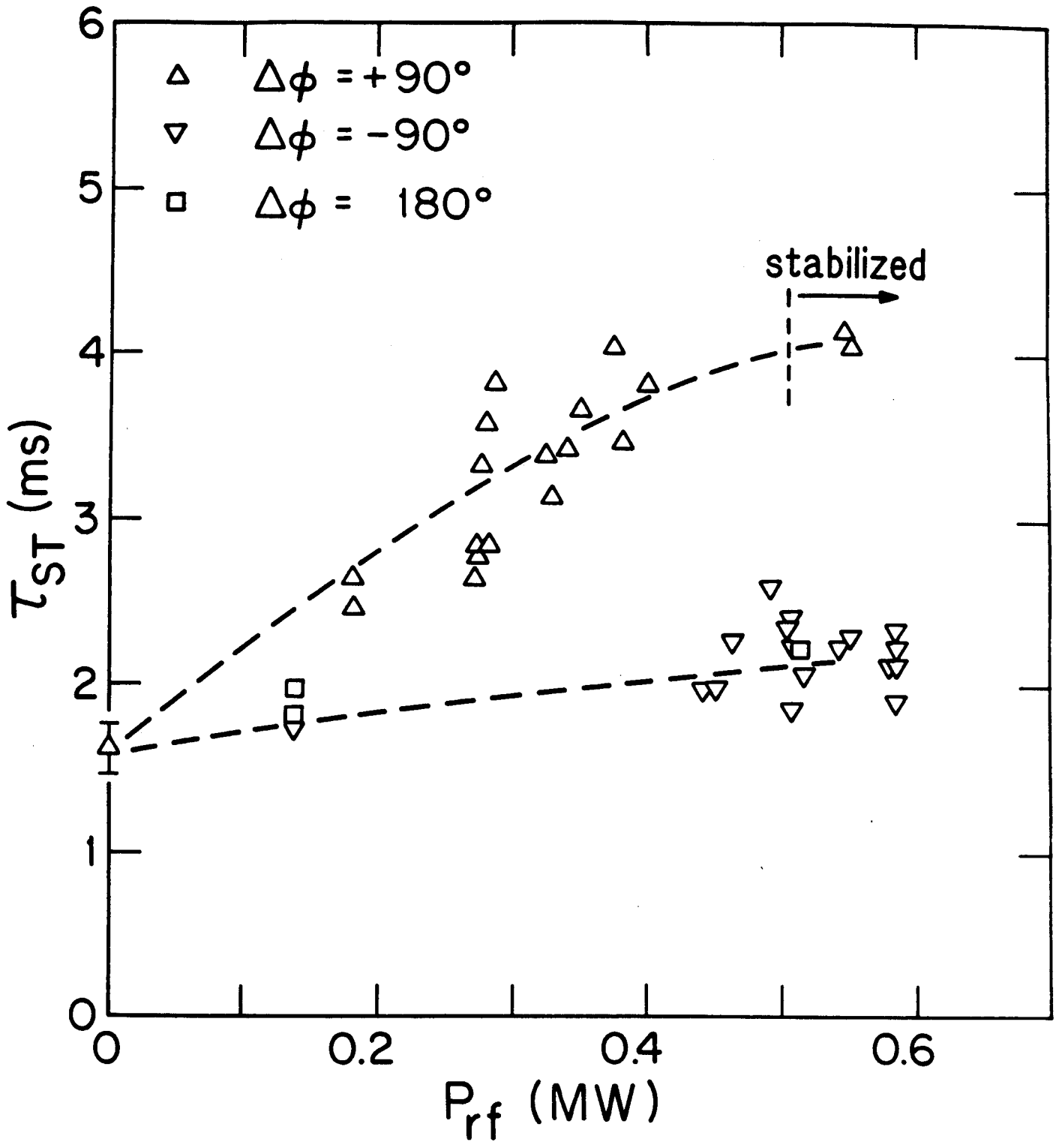

Figure 3

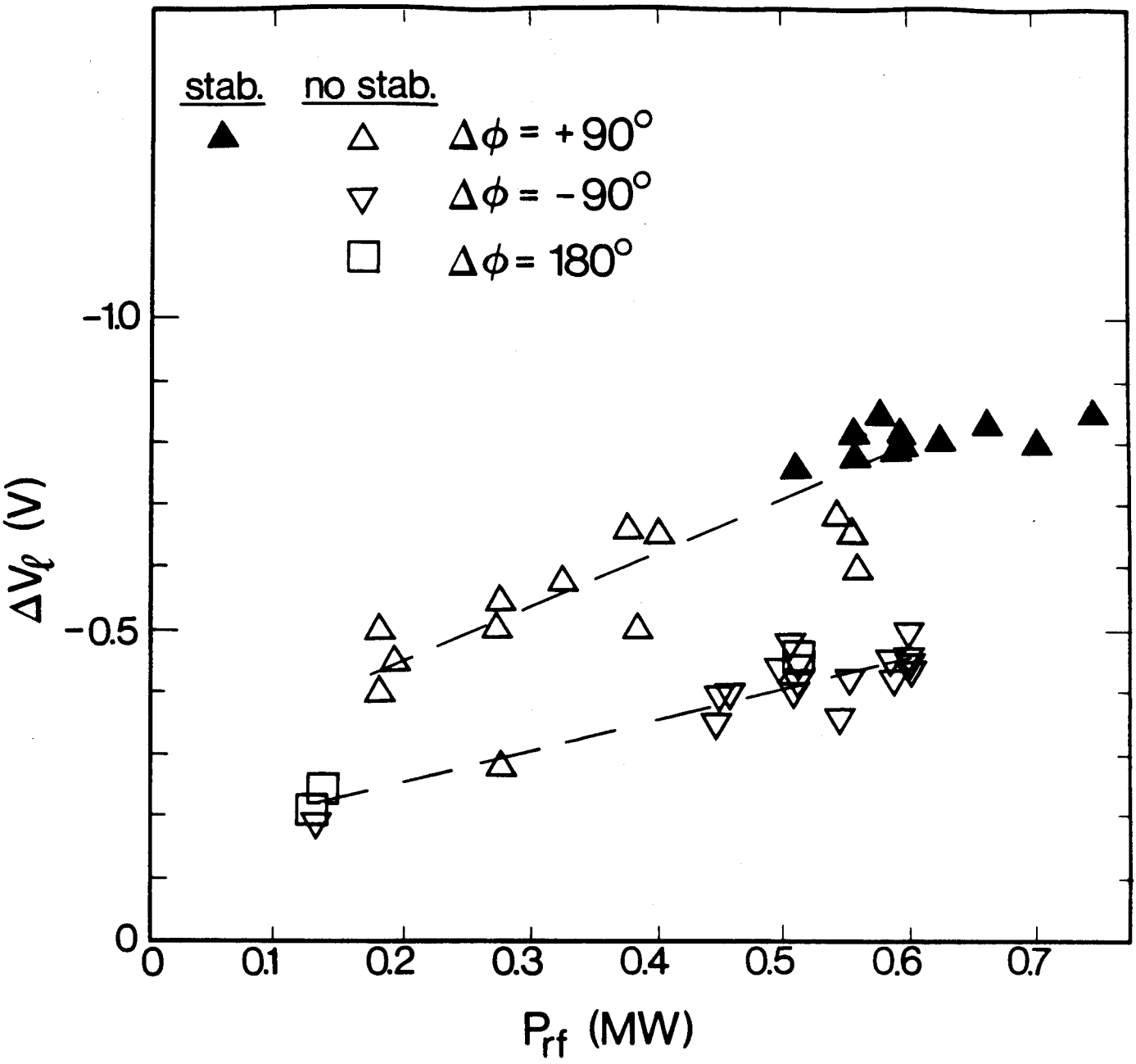
stab.
no stab.
Δφ = +90°
Δφ = -90°
Δφ = 180°
-1.0
-0.5
0
0
0.1
0.2
0.3
0.4
0.5
0.6
0.7
ΔVℓ (V)
Prf (MW)

Figure 4

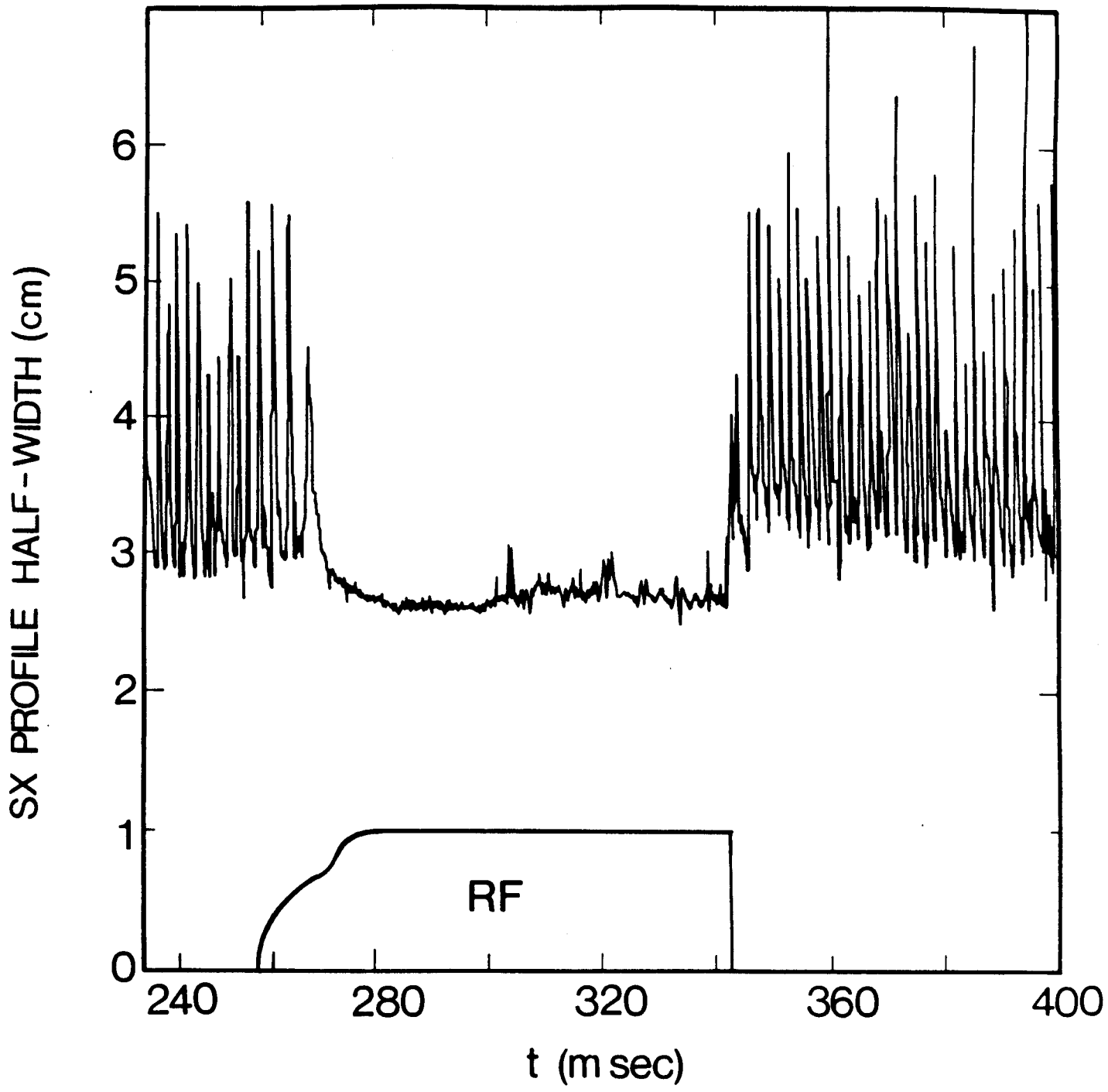

Figure 5

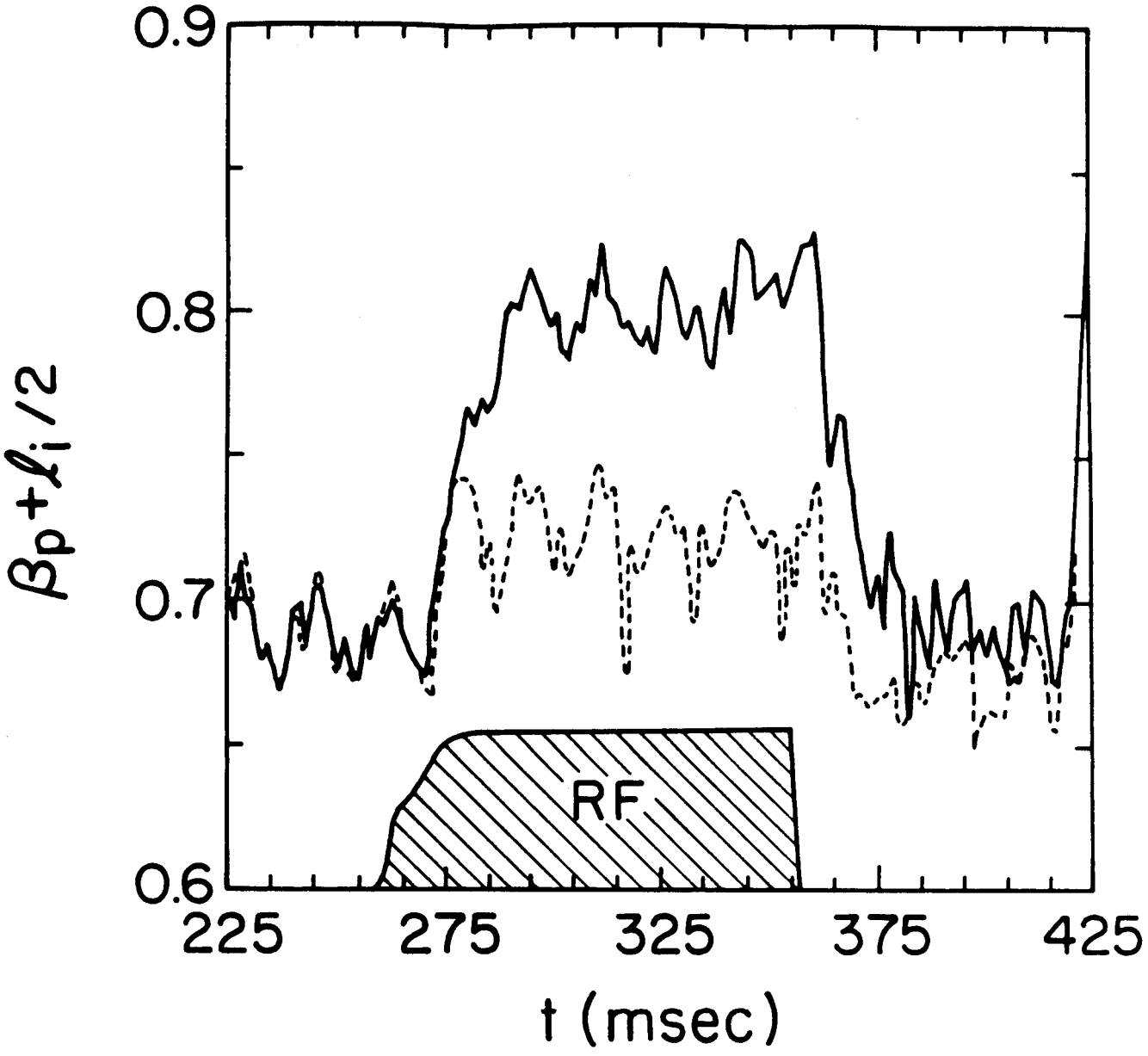

Figure 6

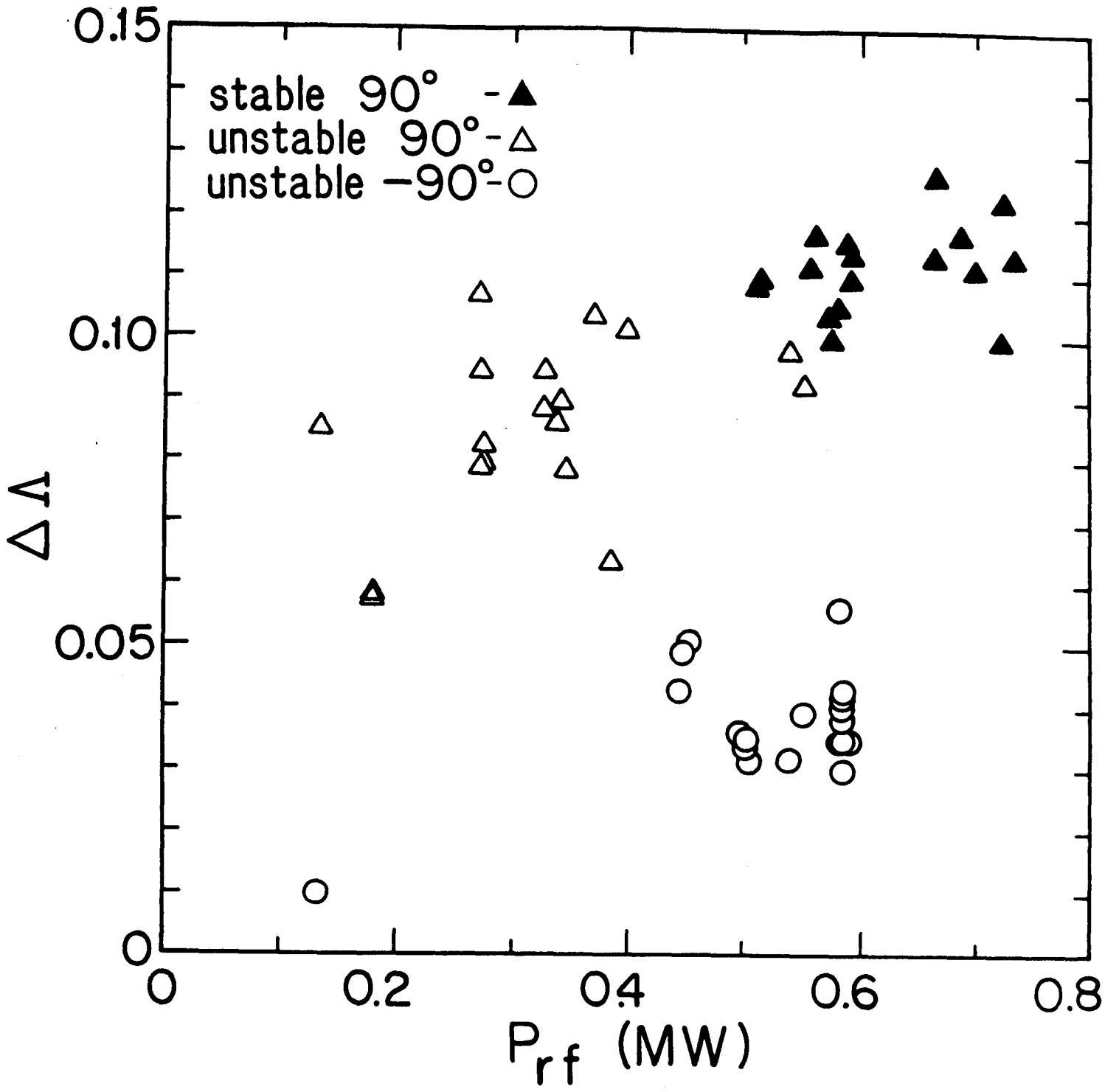
0.15
0.10
0.05
0
stable 90° -▲
unstable 90°-△
unstable −90°-○
Δ Λ
0
0.2
0.4
0.6
0.8
P rf (MW)

Figure 7

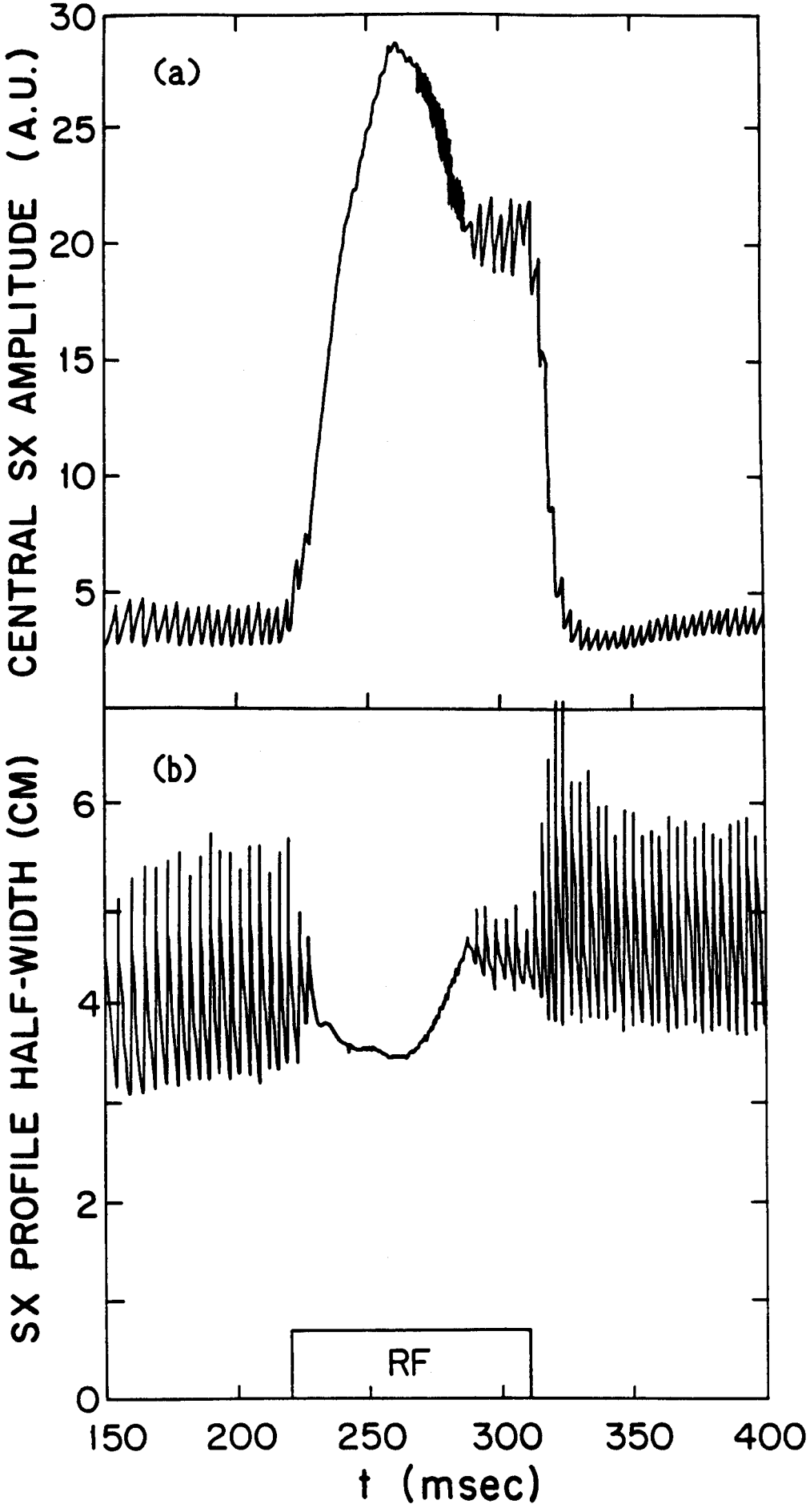
(a)
CENTRAL SX AMPLITUDE (A.U.)
30
25
20
15
10
5
(b)
SX PROFILE HALF-WIDTH (CM)
6
4
2
0
RF
150
200
250
300
350
400
t (msec)

Figure 8

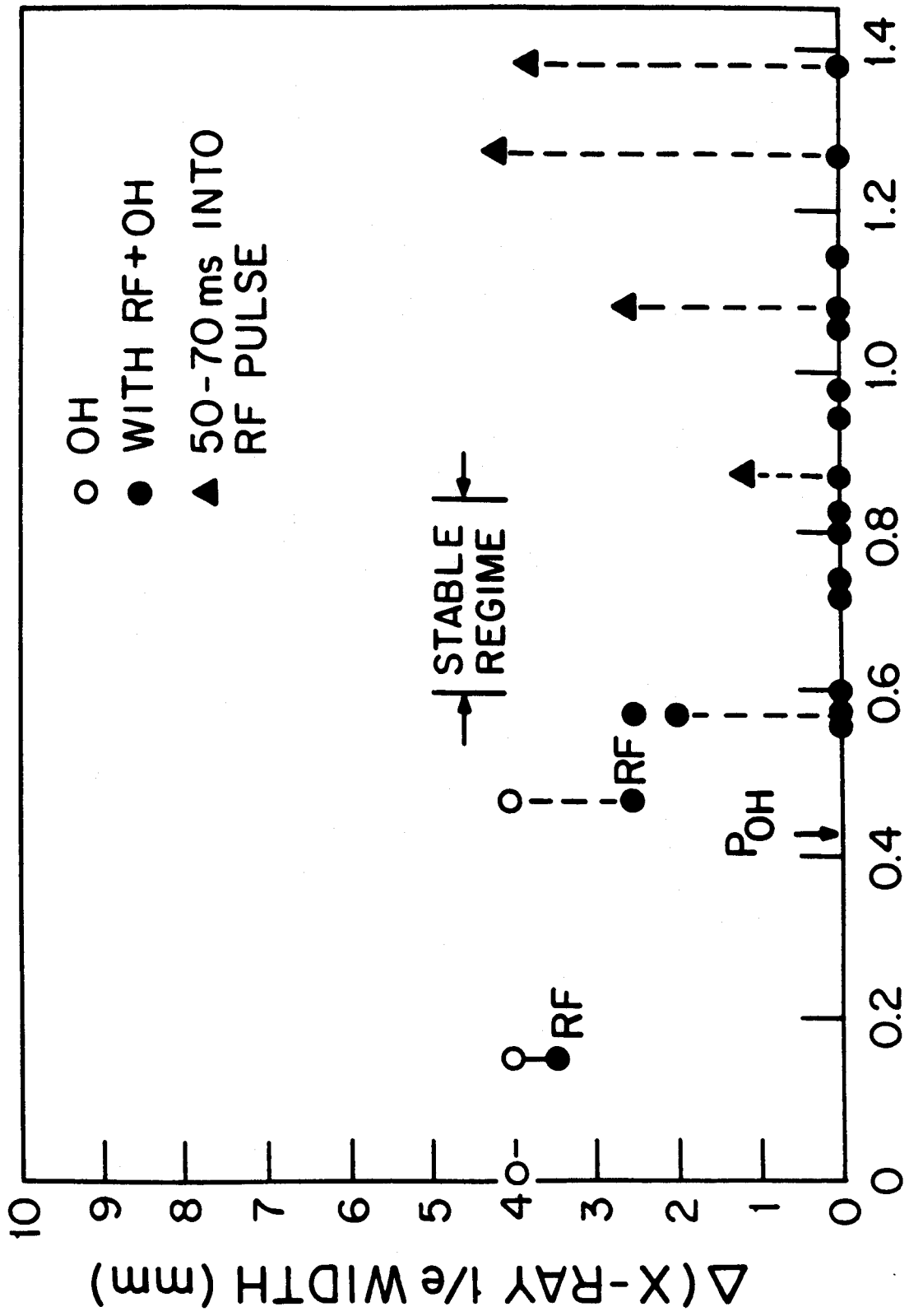
Δ (X-RAY 1/e WIDTH (mm)
10
9
8
7
6
5
4
3
2
1
0
0.2
0.4
0.6
0.8
1.0
1.2
1.4
P_{RF} (MW)
P_{OH}
STABLE REGIME
RF
RF
o OH
● WITH RF+OH
▲ 50-70 ms INTO RF PULSE

Figure 9

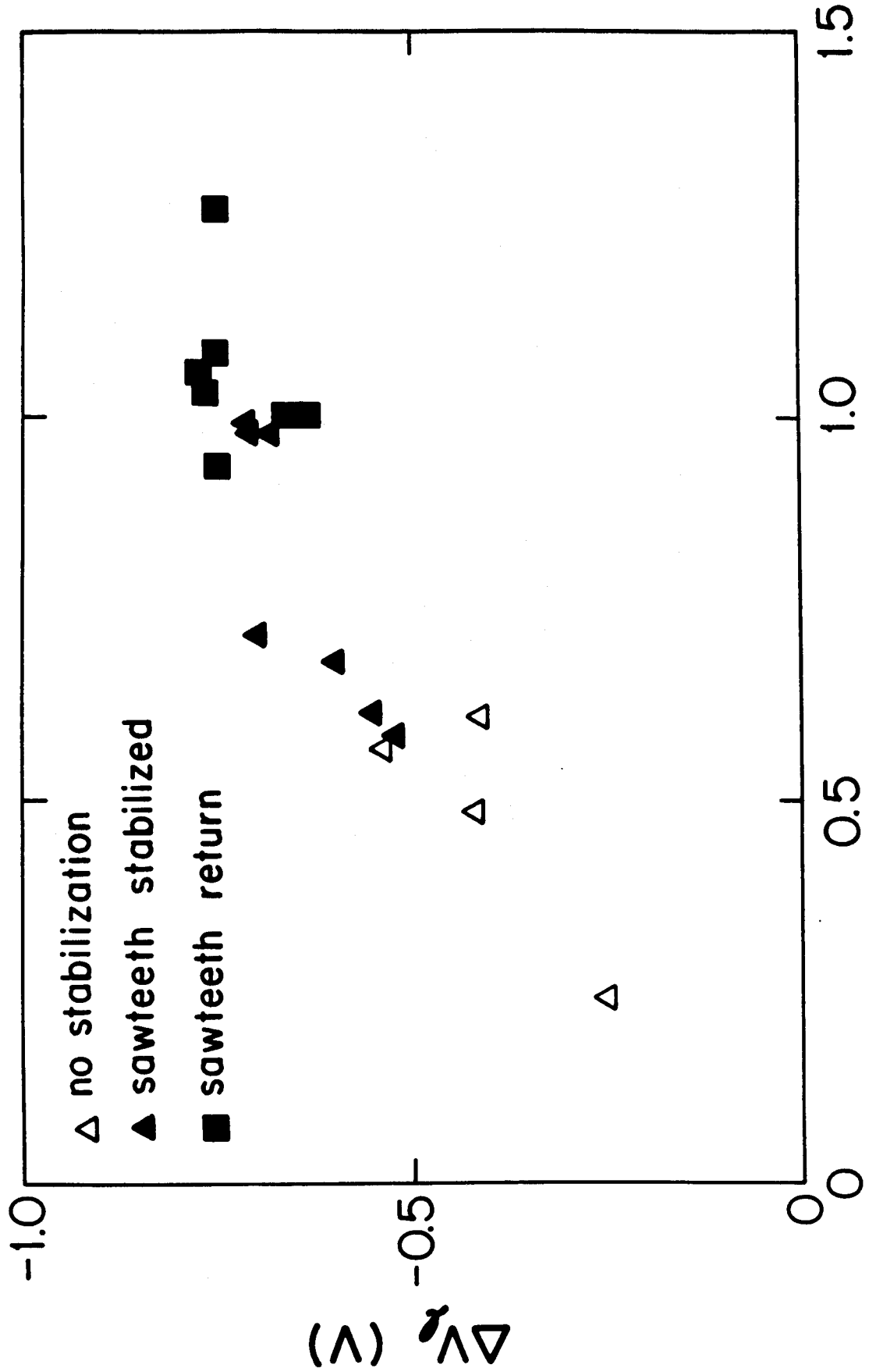
-1.0
-0.5
0
0.5
1.0
1.5
ΔV_g (V)
P_{rf} (MW)
△ no stabilization
▲ sawteeth stabilized
■ sawteeth return

Figure 10